



Original article

The long non-coding RNA landscape of periodontal ligament stem cells subjected to compressive force

Yiping Huang¹, Yingying Zhang², Xiaobei Li¹, Hao Liu¹, Qiaolin Yang¹, Lingfei Jia³, Yunfei Zheng¹ and Weiran Li^{1,4}

¹Department of Orthodontics, Peking University School and Hospital of Stomatology, Beijing, ²Department of Stomatology, Beijing Children's Hospital, Capital Medical University, National Center for Children's Health, Beijing,

³Central Laboratory, Peking University School and Hospital of Stomatology, Beijing, and ⁴National Clinical Research Center for Oral Diseases, National Engineering Laboratory for Digital and Material Technology of Stomatology, Beijing Key Laboratory of Digital Stomatology, Peking University, Beijing, China

Correspondence to: Weiran Li, Department of Orthodontics, Peking University School and Hospital of Stomatology, 22 Zhongguancun South Avenue, Haidian District, Beijing 100081, China. E-mail: weiranli2003@163.com

Summary

Objective: The role of long non-coding ribonucleic acids (lncRNAs) during orthodontic tooth movement remains unclear. We explored the lncRNA landscape of periodontal ligament stem cells (PDLSCs) subjected to compressive force.

Materials and methods: PDLSCs were subjected to static compressive stress (2 g/cm^2) for 12 hours. Total RNA was then extracted and sequenced to measure changes in lncRNA and messenger RNA (mRNA) expression levels. Quantitative real-time polymerase chain reaction (qRT-PCR) was used to validate the expression levels of certain lncRNAs. Differential expression analysis as well as Gene Ontology (GO) and Kyoto Encyclopedia of Genes and Genomes (KEGG) pathway analyses were also performed.

Results: In total, 90 lncRNAs and 519 mRNAs were differentially expressed in PDLSCs under compressive stress. Of the lncRNAs, 72 were upregulated and 18 downregulated. The levels of eight lncRNAs of interest (FER1L4, HIF1A-AS2, MIAT, NEAT1, ADAMTS9-AS2, LUCAT1, MIR31HG, and DHFRP1) were measured via qRT-PCR, and the results were found to be consistent with those of RNA sequencing. GO and KEGG pathway analyses showed that a wide range of biological functions were expressed during compressive loading; most differentially expressed genes were involved in extracellular matrix organization, collagen fibril organization, and the cellular response to hypoxia.

Conclusions: The lncRNA expression profile was significantly altered in PDLSCs subjected to compressive stress. These findings expand our understanding of molecular regulation in the mechanoresponse of PDLSCs.

Introduction

Orthodontic tooth movement is a periodontal tissue remodelling and regeneration process induced by mechanical force (1, 2). Periodontal ligament (PDL) is a periosteum located between alveolar bone and

teeth roots, which possesses the ability to induce bone resorption on the pressure side and bone regeneration on the stretching side during orthodontic treatment (1, 2). Periodontal ligament stem cells (PDLSCs) are tissue-specific stem cells in periodontal tissue (3), which translate

mechanical force into biochemical signals triggering reconstruction of periodontal tissue (4). Compressive force is an important mechanical stimulus on PDLSCs physiologically and traumatically, and a better understanding of how PDLSCs are regulated under compressive stress is essential to improve orthodontic therapeutic approaches.

In recent years, various transcriptional mediators have been shown to involve in mechanical stress transduction process of PDLSCs, including Wnt/β-catenin pathway (5), extracellular signal-regulated kinase (ERK) and mitogen-activated protein kinase (MAPK) pathway (6), phosphatidylinositol 3-kinase (PI3K)/ protein kinase B (Akt)/the mammalian target of rapamycin (mTOR) pathway (7), Hippo-yes-associated protein (YAP)/transcriptional coactivator with PDZ-binding motif (TAZ) signalling pathway (8), and extracellular matrix (ECM) and adhesion molecules (9). These force-sensitive genes respond to biomechanical stimulation and then regulate cell differentiation and periodontal tissue remodelling. Non-coding ribonucleic acids (ncRNAs) account for 98 per cent of all genomic output in humans, serving as important regulatory transcripts in both normal and pathological situations (10). However, little is known of the roles played by such RNAs in response to orthodontic force or orthodontic tooth movement. Recently, the differential microRNA (miRNA) expression profiles of stretched and non-stretched PDLSCs were established using a microarray approach, and 53 tension force-induced differentially expressed miRNAs were identified (11). Of these, miR-21 (12) and miR-29 (13) respond to mechanical stimuli and mediate mechanical force-induced PDLSC differentiation. In contrast, the roles and functions of long non-coding RNAs (lncRNAs), tentatively defined as ncRNAs more than 200 nucleotides in length (14, 15), remain largely unknown in this mechanical transduction process.

lncRNAs are an important class of molecules involved in many biological functions that regulate gene expression via diverse mechanisms (14, 15). A recent study has reported that lncRNA H19 reacts to mechanical tension and mediates mechanical tension-induced osteogenesis of bone marrow mesenchymal stem cells via the focal adhesion kinase (FAK) pathway by sponging miR-138 (16). However, the response of lncRNAs to the mechanical stimulation in PDLSCs remains unclear. Preliminary studies have shown that lncRNAs are involved in the osteoblastic differentiation of PDLSCs (17–19). For example, lncRNA TUG1 facilitates the osteogenic differentiation of PDLSCs via interaction with Lin28A (18). lncRNAs HIF1A-AS1 and HIF1A-AS2 regulate hypoxia-inducible factor (HIF)-1α activity and osteogenic differentiation of periodontal ligament cells (PDLCS) under hypoxia conditions (17). lncRNAs may also mediate mechanical force-induced differentiation of PDLSCs and subsequent periodontal tissue remodelling.

Here, we used RNA sequencing (RNA-seq) to identify differentially expressed lncRNAs and messenger RNAs (mRNAs) in PDLSCs subjected to compressive force. Subsequently, the expression levels of lncRNAs of interest were confirmed via quantitative real-time polymerase chain reaction (qRT-PCR). Finally, we investigated the potential regulatory roles played by differentially expressed genes via Gene Ontology (GO) and Kyoto Encyclopedia of Genes and Genomes (KEGG) pathway analyses. The findings improve our understanding of how PDLSCs respond to compressive stress.

Materials and methods

Ethical approval

The study protocol was approved by the ethics committee of Peking University School of Stomatology (approval no. PKUSSIRB-2011007).

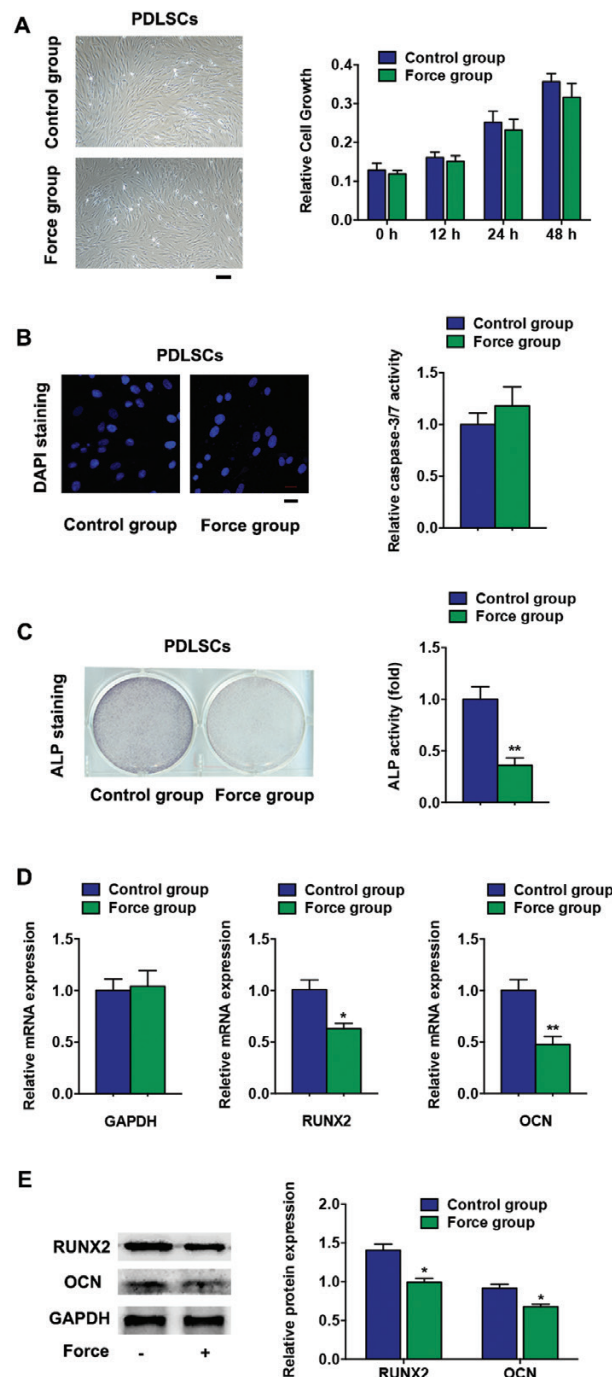


Figure 1. Compressive force inhibited the osteoblastic differentiation of periodontal ligament stem cells (PDLSCs). (a) Left: cell morphology images of PDLSCs with or without compressive force for 12 hours. Scale bar, 200 µm. Right: relative cell growth of these PDLSCs. (b) Left: 4',6-diamidino-2-phenylindole (DAPI) staining of PDLSCs with or without compressive force. Scale bar, 50 µm. Right: relative caspase-3/7 activity of these PDLSCs. (c) Left: alkaline phosphatase (ALP)-stained images of PDLSCs exposed to compressive force or not. Right: histograms of the normalized ALP activities of these PDLSCs. (d) Relative messenger RNA (mRNA) expression levels of glyceraldehyde 3-phosphate dehydrogenase (GAPDH), runt-related transcription factor 2 (RUNX2), and osteocalcin (OCN) as determined by quantitative real-time polymerase chain reaction (qRT-PCR) analysis in PDLSCs exposed or not to compressive force [normalized to peptidylprolyl isomerase B (PPIB)]. (e) Western blot analysis (left) and quantification (right) of RUNX2, OCN, and GAPDH expression in these PDLSCs. Results are presented as mean ± standard deviation (* $P < 0.05$, ** $P < 0.01$).

Cell culture

Human PDLSCs were isolated, cultured, and characterized as described previously (20). The cells were cultured in α -Modified Eagle's Medium (Gibco, Grand Island, New York, USA) supplemented with 10 per cent (v/v) fetal bovine serum (Gibco) and 1 per cent penicillin/streptomycin (Invitrogen, Carlsbad, California, USA) in a humidified atmosphere at 37°C under 5 per cent (v/v) CO₂.

Mechanical stimulation: application of a static compressive force

PDLSCs were seeded into six-well plates. After 80 per cent confluence was attained, a cover glass and a glass bottle containing steel balls were placed on the cells. The compressive force was adjusted to 2 g/cm², as described in previous studies (21, 22), and maintained for 12 hours. Control PDLSCs were cultured without compression.

Cell viability

Cell viability assay was measured using a cell counting kit (CCK-8; Dojindo, Kumamoto, Japan). Briefly, after exposure to compressive stress for 12 hours, the cells were seeded into each well of a 96-well plate. At the scheduled time (0, 12, 24, and 48

hours), CCK-8 reagent was added to each well and incubated at 37°C for 3 hours. Absorbance values at 450 nm were measured using a microplate spectrophotometer (Bio-Tek Instruments Inc., Winoski, Vermont, USA).

Immunofluorescence staining

Immunofluorescence staining was performed as described previously (23). Cells grown on glass coverslips were subjected to compressive force for 12 hours. The cells were washed, fixed with 4 per cent (v/v) paraformaldehyde, and stained with 4',6-diamidino-2-phenylindole (DAPI). Images were captured with a confocal imaging system (Carl Zeiss, Jena, Germany).

Caspase-3/7 activity

The cellular enzymatic activity of caspase-3/7 was determined using a colorimetric assay kit (Caspase-Glo 3/7 Assay Systems; Promega, Madison, Michigan, USA) according to the manufacturer's protocol. Briefly, after exposure to compressive force, cells were lysed and incubated with a luminogenic substrate, which is cleaved by activated caspase-3/7 in apoptotic cells. After incubation for 1 hour, luminescence was quantified using a Centro XS³ LB 960 luminometer (Berthold, Bad Wildbad, Germany).

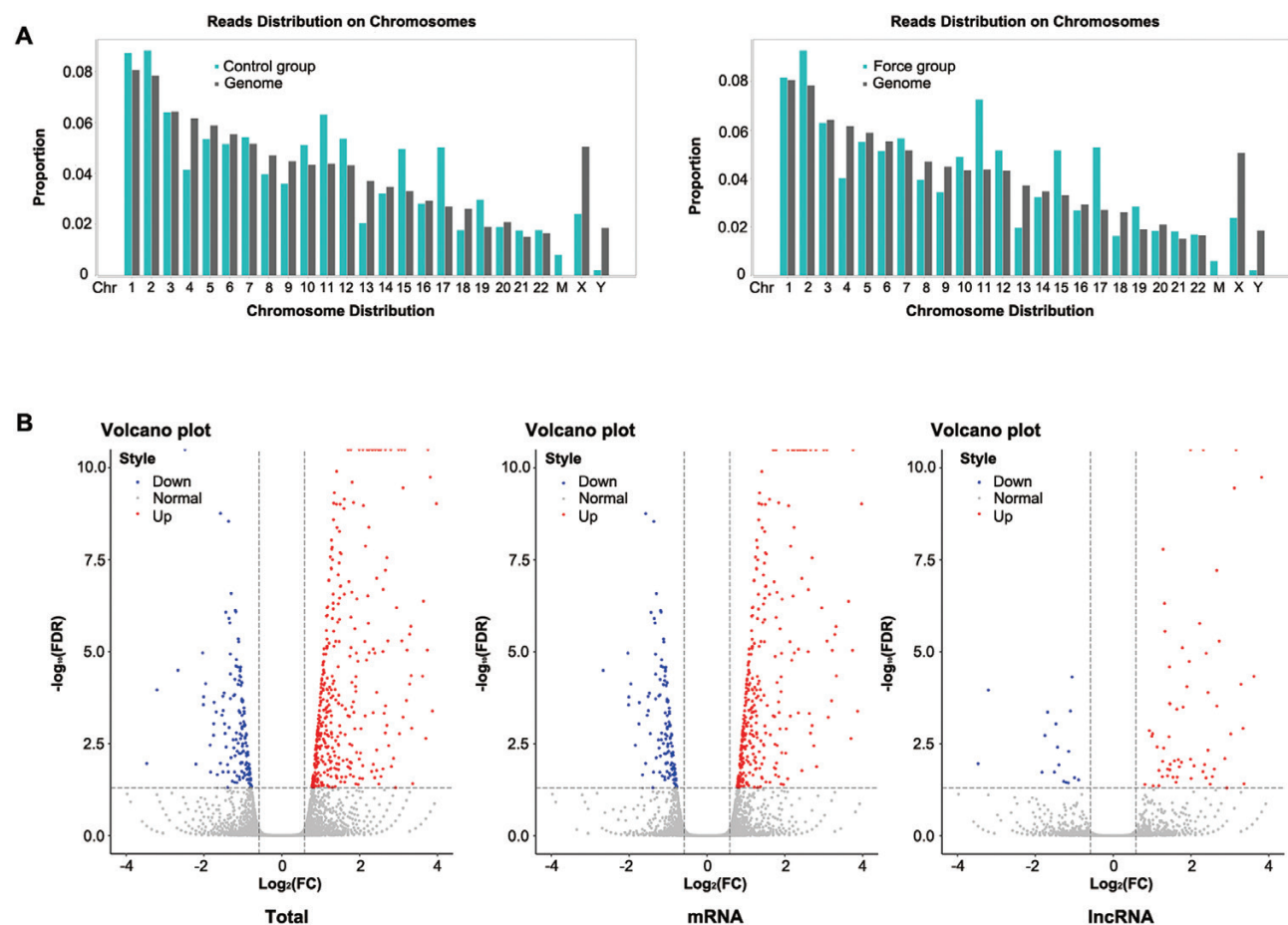


Figure 2. Differential expression of long non-coding ribonucleic acids (lncRNAs) and messenger RNAs (mRNAs) in periodontal ligament stem cells (PDLSCs) subjected to compressive force. (a) Chromosomal read distributions of control PDLSCs (left) and PDLSCs subjected to compressive force for 12 hours (right). (b) Volcano plots of differentially expressed mRNAs and lncRNAs. Red points (fold changes greater than 1.5): upregulated mRNAs or lncRNAs; blue points (fold changes less than 0.6667): downregulated mRNAs or lncRNAs.

Alkaline phosphatase staining and activity

Alkaline phosphatase (ALP) staining and activity were assessed as described previously (23). ALP staining was performed using an nitroblue tetrazolium (NBT)/5-bromo-4-chloro-3-indolyl-phosphate (BCIP) kit (CoWin Biotech, Beijing, China) according to the manufacturer's protocol. Briefly, cultured cells were fixed in 4 per cent (v/v) paraformaldehyde for 30 minutes and stained with an alkaline solution for 20 minutes at 37°C in dark. ALP activity was analysed using a colorimetric assay kit (Biovision, Milpitas, California, USA). Cells were rinsed with phosphate-buffered saline, followed by 1 per cent (v/v) Triton X-100, scraped into distilled water, and subjected to three cycles of freezing and thawing. ALP activity was determined by absorbance at 405 nm using *p*-nitrophenyl phosphate as the substrate. Total protein content was determined using the bicinchoninic acid (BCA) method of the Pierce BCA Protein Assay Kit (Thermo Fisher Scientific, Waltham, Massachusetts, USA). ALP activities relative to those of the control were calculated after normalization to total protein content.

RNA isolation and qRT-PCR

Total RNA was extracted using TRIzol reagent (Invitrogen) according to the manufacturer's instructions and reverse-transcribed into cDNA using a cDNA Reverse Transcription Kit (Takara, Tokyo, Japan). The primers were designed using Primer 5 software according to Minimum Information for Publication of Quantitative Real-Time PCR Experiments (MIQE) guidelines (24) (Supplementary Table 1). The primer and target/amplicon information for the investigated genes are listed in Supplementary Table 2. The primer specificity and qRT-PCR efficiencies were confirmed. qRT-PCR was performed on 1 µg RNA using the SYBR Green PCR Master Mix on an ABI

Prism 7500 Real-Time PCR System (Applied Biosystems, Foster City, California, USA). The following settings were used: 95°C for 10 minutes followed by 40 cycles of 95°C for 15 seconds and 60°C for 1 minute. The glyceraldehyde 3-phosphate dehydrogenase (GAPDH) and peptidylprolyl isomerase B (PPIB) served as the internal control. Data were analysed using the $2^{-\Delta\Delta CT}$ relative expression method, as described previously (23).

Western blot

Western blot was performed as described previously (23). Briefly, cells were harvested, washed, and lysed in radioimmunoprecipitation assay buffer. Protein content was determined using the BCA method (Thermo Fisher Scientific). Proteins were separated via 12 per cent (w/v) sodium dodecyl sulphate–polyacrylamide gel electrophoresis and electroblotted to polyvinylidene fluoride membranes. After blocking, proteins were detected by overnight incubation with primary antibodies against osteocalcin (OCN; Abcam, Cambridge, UK), runt-related transcription factor 2 (RUNX2; Abcam), and GAPDH (Zhongshan Goldenbridge, Beijing, China) at dilutions of 1:1000. After washing, the membranes were incubated with secondary antibodies (Zhongshan Goldenbridge; 1:10 000 dilution) at room temperature for 1 hour. Specific complexes were visualized using an enhanced chemiluminescence kit (Applygen, Beijing, China). Band intensities were quantified using ImageJ software (<http://rsb.info.nih.gov/ij/>). The background was subtracted and the signal of each target band was normalized to that of GAPDH.

lncRNA and mRNA sequencing

As described previously, 4 µg RNA was treated with DNase (Qiagen, Hilden, Germany) (20). Ribosomal RNA (rRNA) was

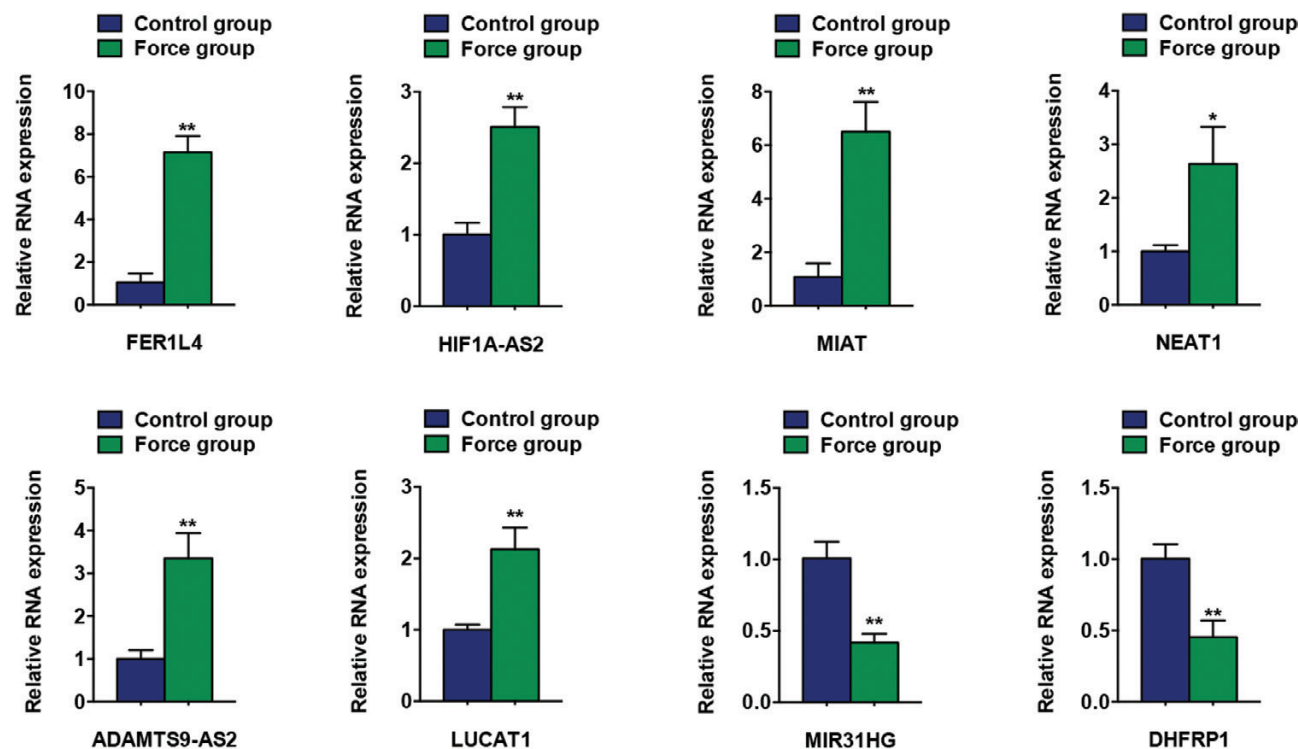


Figure 3. Differentially expressed long non-coding ribonucleic acids (lncRNAs) (FER1L4, HIF1A-AS2, MIAT, NEAT1, ADAMTS9-AS2, LUCAT1, MIR31HG, and DHFRP1), the levels of which were validated by quantitative real-time -polymerase chain reaction [qRT-PCR; normalized to glyceraldehyde 3-phosphate dehydrogenase (GAPDH)]. Results are presented as mean \pm standard deviation (* $P < 0.05$, ** $P < 0.01$).

depleted using a Ribo-Zero Magnetic Kit (Illumina, San Diego, California, USA) and an RNA library prepared using an Illumina kit. Paired-end sequencing was performed with the aid of a HiSeq 2000 system (Illumina). Whole transcriptome sequencing data were filtered using domestic java code (removing the adaptor sequences, reads with more than 5 per cent ambiguous bases and low-quality reads containing more than 20 per cent of bases with qualities of less than 20 per cent). The trimmed data were then mapped to the human genome (hg19) using HISAT2 (25). We used HTseq (26) to count the genes and calculated the reads per kilobase transcriptome per million mapped reads (RPKM) to evaluate the gene expression level. Genes with normalized RPKM values more than or equal to 1 in at least one sample were subjected to analysis.

Bioinformatics

Differential gene expression analysis was performed using the EBSeq package (27) of the Bioconductor R program, as described previously (20). In the output file of EBSeq result, false discovery rate (FDR) was applied using Benjamini and Hochberg algorithm (28) based on the *P*-value. We defined the differentially expressed genes under the criteria as follows: 1. Fold change greater than 1.5 or fold change less than 0.6667, and 2. FDR less than 0.05. The Database for Annotation, Visualization and Integrated Discovery (29) was used for GO and KEGG pathway analyses. The high-throughput data were uploaded and the enriched biological GO terms and the KEGG pathways were identified by this gene annotation enrichment tool.

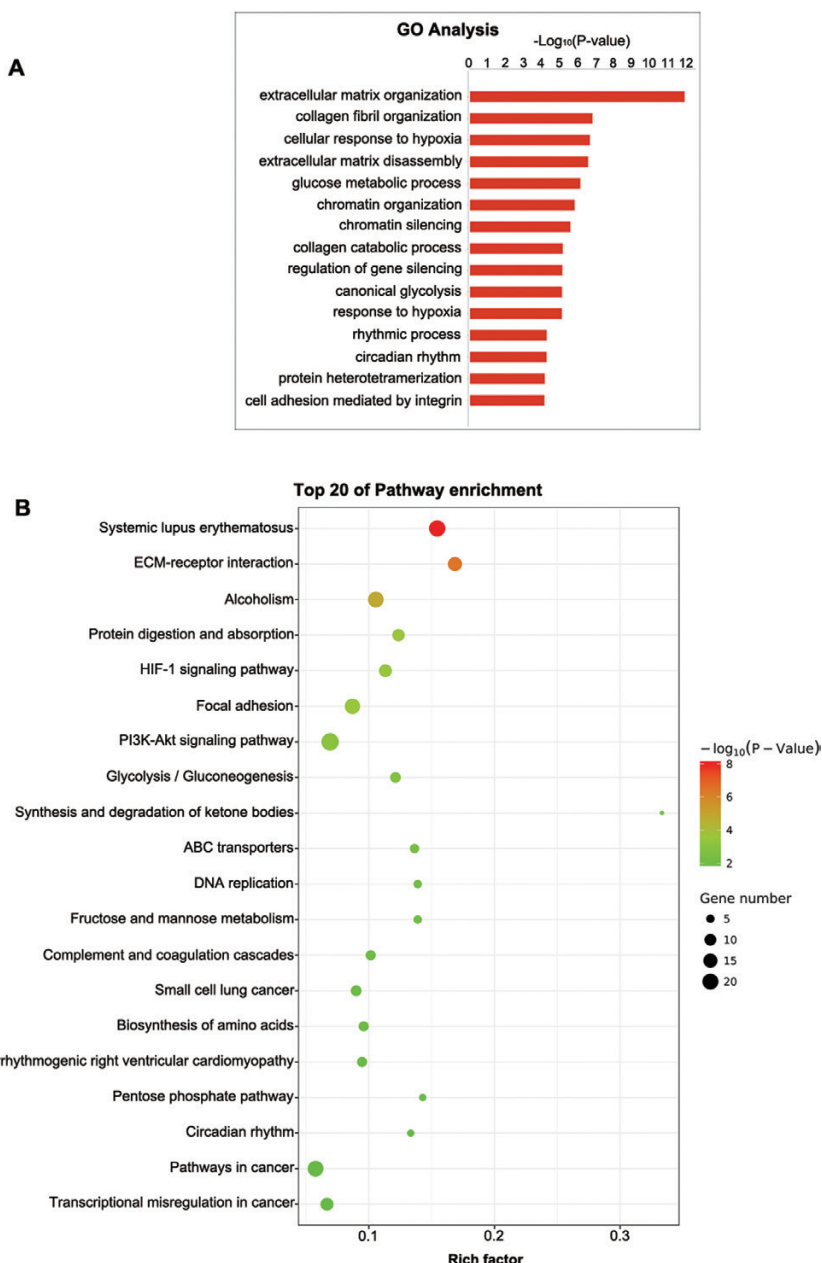


Figure 4. Gene Ontology (GO) term enrichment and Kyoto Encyclopedia of Genes and Genomes (KEGG) pathway analyses. (a) The top 15 GO enrichments. (b) The top 20 KEGG pathway enrichments.

Statistics

All statistical analyses were performed with SPSS software (IBM, Armonk, New York, USA). The quantitative data are expressed as means \pm standard deviation. The one-sample Kolmogorov–Smirnov test was used to confirm the normality of the quantitative data. For the qRT-PCR, ALP activity, western blot quantification, CCK-8, and caspase-3/7 activity assay, differences between two groups were analysed using Student's *t*-test. A *P*-value less than 0.05 was considered statistically significant.

Results

Compressive force inhibited the osteoblastic differentiation of PDLSCs

PDLSCs subjected to compressive force for 12 hours exhibited no significant morphological change (Figure 1a). CCK-8 assay showed

that no significant difference of cell growth was detected between the force group and the control group (three samples, three technical replicates per sample; Figure 1a). DAPI staining and caspase-3/7 activity assay confirmed the absence of increased apoptosis in the force group (three samples, three technical replicates per sample; Figure 1b). However, ALP staining and activity, early markers of osteogenic differentiation, were inhibited by the compressive force (three samples, three technical replicates per sample; Figure 1c). The GAPDH expression remained stable relative to PPIB and thus served as internal control in subsequent experiments. The mRNA expression of the osteogenic genes RUNX2 and OCN was inhibited under compressive force (three samples, three technical replicates per sample; Figure 1d). Western blot also confirmed the downregulation of protein expression of RUNX2 and OCN under compression (three samples, three technical replicates per sample; Figure 1e and Supplementary Figure 1).

ECM-receptor Interaction

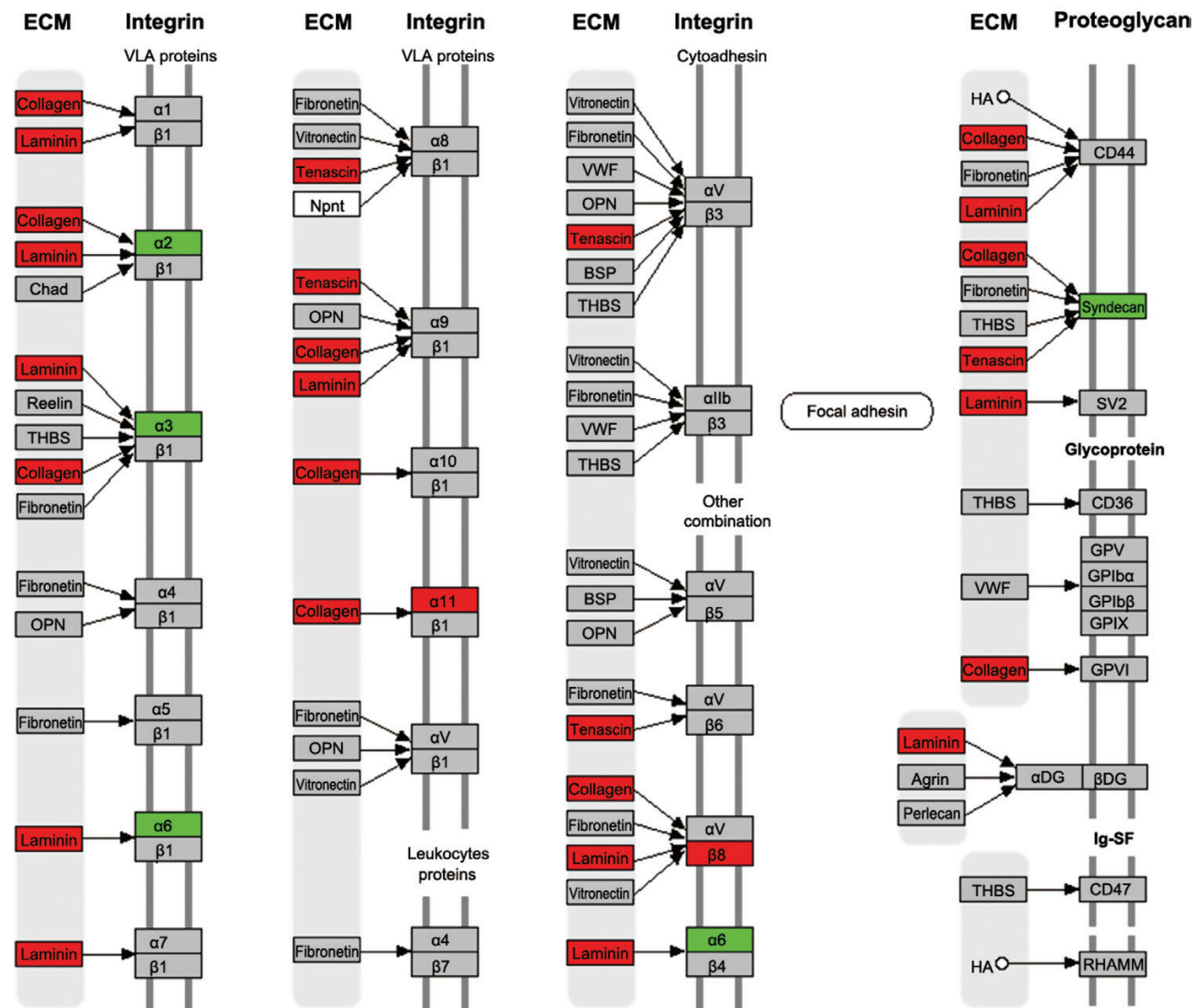


Figure 5. Kyoto Encyclopedia of Genes and Genomes (KEGG) map of genes involved in extracellular matrix (ECM)–receptor interaction pathway. Red squares: significantly upregulated genes; green squares: significantly downregulated genes.

Differential expression of lncRNAs and mRNAs in PDLSCs subjected to compressive force

rRNA-depleted RNA-seq detected 4029 lncRNAs in control cells and 4065 in PDLSCs subjected to compressive force. Also, 10 231 mRNAs (control group) and 10 254 mRNAs (force group) were annotated. The lncRNAs were broadly distributed across the 24 pairs of human chromosomes (Figure 2a). The differential expressions of lncRNAs and mRNAs are visually displayed on volcano plots (one sample; Figure 2b). A total of 90 lncRNAs and 519 mRNAs were differentially expressed, with FDR less than 0.05 and fold change greater than 1.5 or fold change less than 0.6667. Of the differentially expressed lncRNAs, 72 were upregulated and 18 downregulated by compressive stress. Of the differentially expressed 519 mRNAs, 373 were upregulated and 146 downregulated.

Validation of differentially expressed lncRNAs

To validate the RNA-seq results, eight candidate lncRNAs with significant fold change were subjected to qRT-PCR analysis (FER1L4, HIF1A-AS2, MIAT, NEAT1, ADAMTS9-AS2, LUCAT1, MIR31HG, and DHFRP1). Compared with controls, PDLSCs subjected to compressive force exhibited increased expression of FER1L4, HIF1A-AS2, MIAT, NEAT1, ADAMTS9-AS2, and LUCAT1, and decreased expression of MIR31HG and DHFRP1 (five samples, three technical replicates per sample; Figure 3). All results were consistent with the normalized RNA-seq data.

GO and KEGG enrichment analyses

GO and KEGG pathway analyses were used to functionally analyse the differentially expressed mRNA and derive functional information on the biological processes and pathways affected by compressive stimulus. The GO results showed that ECM organization, collagen fibril organization, ECM disassembly, the cellular response to hypoxia, chromatin organization, and chromatin silencing were the top six significantly enriched GO terms (Figure 4a). Of these, GO:0030198 (ECM organization) was significantly enriched in terms of mRNAs (36 in number). KEGG enrichment analysis showed that 30 pathways were significantly affected in terms of differentially expressed genes, including ECM–receptor interaction, focal adhesion, HIF-1 signalling pathway, PI3K/Akt signalling pathway, protein digestion and absorption, and glycolysis/gluconeogenesis (Figure 4b). We created a diagram showing the genes affected by compressive stress in terms of ECM–receptor interaction (Figure 5), HIF-1 signalling pathway (Figure 6), and PI3K/Akt signalling pathway (Figure 7). Differentially expressed genes are colour coded.

Discussion

We explored the lncRNA and mRNA expression profiles of PDLSCs subjected to compressive stress and found that such PDLSCs exhibited decreased osteogenic differentiation, and 90 lncRNAs and 519 mRNAs were differentially expressed in compressed PDLSCs compared with normal cells. Over the past decades, the molecular

HIF-1 signalling pathway

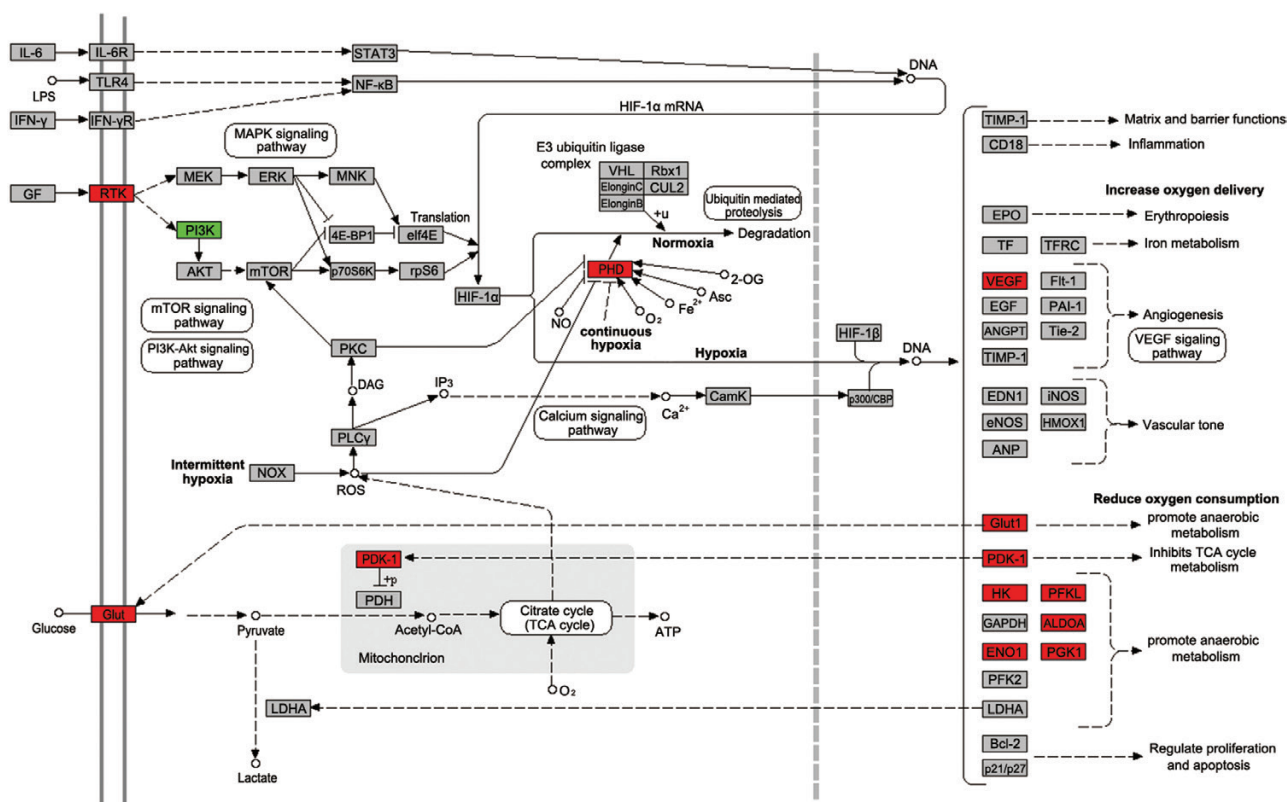


Figure 6. Kyoto Encyclopedia of Genes and Genomes (KEGG) map of genes involved in hypoxia-inducible factor (HIF)-1 signalling pathway. Red squares: significantly upregulated genes; green squares: significantly downregulated genes.

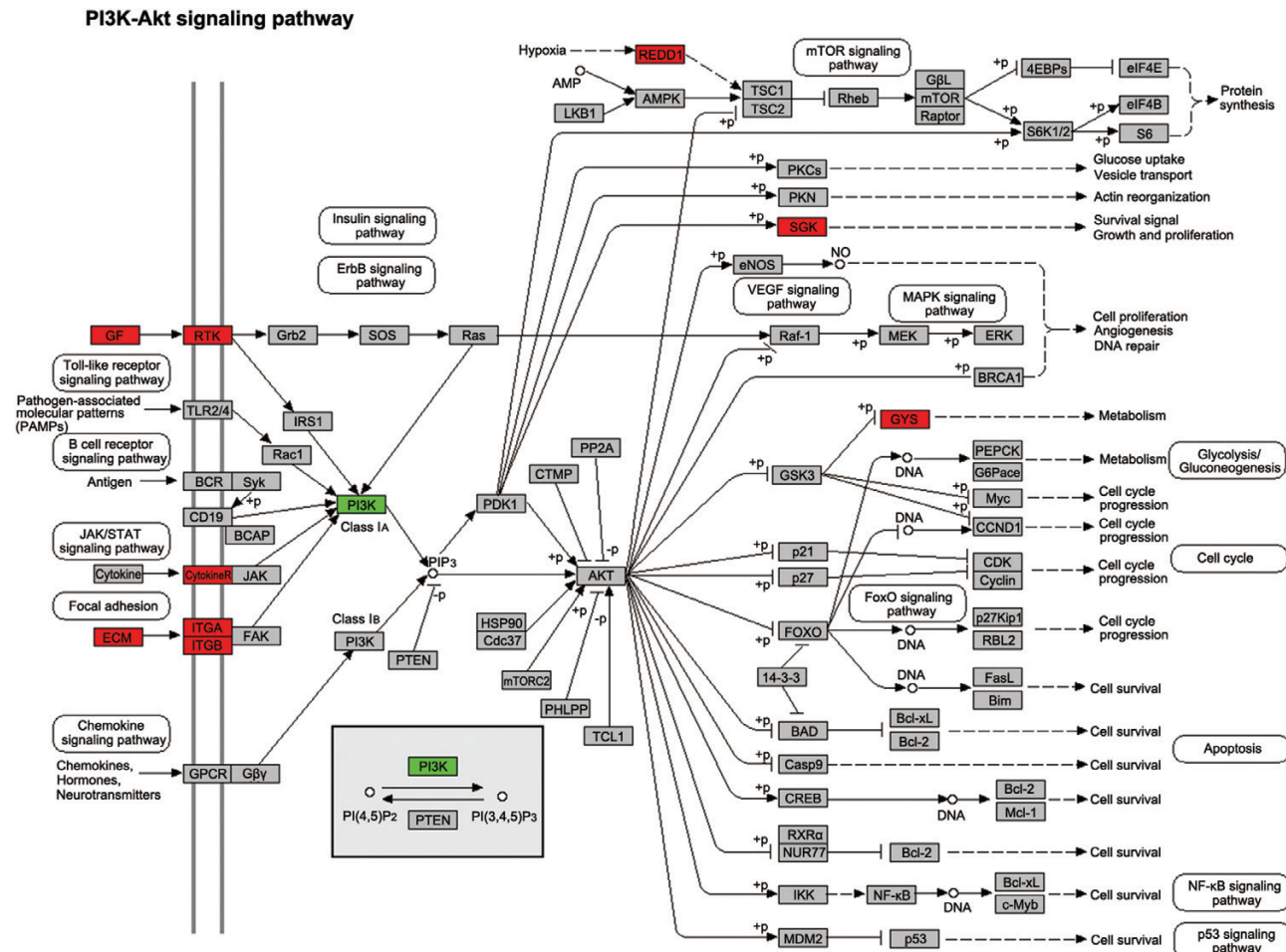


Figure 7. Kyoto Encyclopedia of Genes and Genomes (KEGG) map of genes involved in phosphatidylinositol 3-kinase (PI3K)/ protein kinase B (Akt) signalling pathway. Red squares: significantly upregulated genes; green squares: significantly downregulated genes.

mechanisms of orthodontic tooth movement have been extensively studied (1, 2). However, our understanding of the mechanical-chemical transduction process remains incomplete. In recent years, lncRNAs have received a great deal of attention because of their regulatory roles (14, 15), but the functional characterization of lncRNAs involved in periodontal tissue remodelling caused by orthodontic force has not been explored systematically. Some recent studies have explored differential miRNA expression of PDLSCs under tension stimulation (11, 30). Among them, miR-21 responds to orthodontic force applied to periodontal tissue in a dose- and time-dependent manner, and regulates PDLSC osteogenesis following orthodontic tooth movement (12). miR-29 directly regulates ECM-encoding genes in loaded PDLSCs (13). These studies reveal a mechanism that miRNAs modulate orthodontic tooth movement and tissue remodelling. Similarly, our finding that 90 lncRNAs were differentially expressed on application of compressive stress suggests that lncRNAs may trigger mechanical force-induced variations in PDLSC functions.

On the basis of RNA-seq results, we chose candidate lncRNAs for further validation. Eight lncRNAs (FER1L4, HIF1A-AS2, MIAT, NEAT1, ADAMTS9-AS2, LUCAT1, MIR31HG, and DHFRP1) that possessed significant fold change and have been reported to play important roles in biological function were subjected to qRT-PCR analysis. The results were consistent with the RNA-seq data. Of these,

HIF1A-AS2, MIAT, and MIR31HG have been reported to regulate the osteogenic differentiation of mesenchymal stem cells. HIF1A-AS2 is complementary to HIF-1 α mRNA and inhibits HIF-1 α expression and osteogenic differentiation of PDLSCs under hypoxia conditions (17). MIAT expression decreases in a time-dependent manner during osteogenesis, and knock-down of MIAT promotes the osteogenic differentiation of stem cells (31). MIR31HG participates in nuclear factor- κ B (NF- κ B) activation and is involved in osteogenesis under both normal and inflammatory conditions (32). Our present results indicate that these lncRNAs may also respond to mechanical stress, mediating the force-induced osteogenic differentiation of PDLSCs during orthodontic tooth movement. There are few data about the role of ADAMTS9-AS2, FER1L4, LUCAT1, and DHFRP1 in stem cell differentiation, and most have been studied in the context of cancer research. ADAMTS9-AS2 is an antisense transcript of ADAMTS9 (33), which encodes a metalloprotease, indicating that ADAMTS9-AS2 may interact with ADAMTS9 to modulate ECM activity during periodontal tissue remodelling. However, among the differentially expressed lncRNAs, most of them were uncharacterized and need further investigation. In addition, we used GAPDH as internal control in the qRT-PCR analysis. Previous study showed that the stably expressed reference gene for normalization is PPIB in PDL fibroblasts under compressive condition using geNorm mathematical algorithms (34). However, we found that the expression of

GAPDH remained stable and did not change significantly relative to PPIB in PDLSCs subjected to compressive force. Thus, we used GAPDH as internal control in subsequent experiments.

GO analysis showed that a wide range of functions were significantly enriched during compressive loading, including ECM organization, collagen fibril organization, ECM disassembly, and the cellular response to hypoxia. The enriched pathways were involved in ECM–receptor interaction, focal adhesion, HIF-1 signalling pathway, and PI3K/Akt signalling pathway. The degeneration and reconstruction of ECM components play important roles in orthodontic tooth movement (1, 9). The ECM is a complex mixture of structural and functional macromolecules, and specific interactions between cells and the ECM control cellular activities including adhesion, differentiation, proliferation, and apoptosis, which are all involved in tissue remodelling (35, 36). In addition, the cellular response to hypoxia was affected by compressive stress. Tooth loading triggers local hypoxia in compressed areas (1). Previous studies have found that hypoxia significantly enhances HIF-1 α and active HIF-1 α significantly increases receptor activator of nuclear factor- κ B ligand (RANKL) expression and enhances osteoclastogenesis on the compression side of PDL (37), indicating the role of hypoxia in periodontal tissue remodelling. We finally created KEGG maps of genes targeted during compressive loading in terms of ECM–receptor interaction, HIF-1 signalling pathway, and PI3K/Akt signalling pathway. However, further study regarding the relation between the differentially expressed lncRNAs and these enriched biological themes is needed to disclose the function and mechanism of the regulated lncRNAs under compressive force.

In summary, compressed PDLSCs exhibited an lncRNA expression profile different from that of normal PDLSCs: 72 lncRNAs were upregulated and 18 downregulated. Changes in the levels of eight lncRNAs of interest were validated. The key biological processes and pathways affected were identified. Our work may inspire further investigation into how lncRNAs transduce mechanical force.

Supplementary material

Supplementary data are available at *European Journal of Orthodontics* online.

Funding

The National Natural Science Foundation of China (81670957 to LW, 81700938 to ZY) and the Fund for Fostering Young Scholars of Peking University Health Science Center (BMU2017PY022).

Conflict of interest

None declared.

References

1. Feller, L., Khammissa, R.A., Schechter, I., Moodley, A., Thomadakis, G. and Lemmer, J. (2015) Periodontal biological events associated with orthodontic tooth movement: the biomechanics of the cytoskeleton and the extracellular matrix. *The Scientific World Journal*, 2015, 894123.
2. Krishnan, V. and Davidovitch, Z. (2006) Cellular, molecular, and tissue-level reactions to orthodontic force. *American Journal of Orthodontics and Dentofacial Orthopedics*, 129, 469.e1–469.e32.
3. Seo, B.M., Miura, M., Gronthos, S., Bartold, P.M., Batouli, S., Brahim, J., Young, M., Robey, P.G., Wang, C.Y. and Shi, S. (2004) Investigation of multipotent postnatal stem cells from human periodontal ligament. *Lancet*, 364, 149–155.
4. Zhang, L., Liu, W., Zhao, J., Ma, X., Shen, L., Zhang, Y., Jin, F. and Jin, Y. (2016) Mechanical stress regulates osteogenic differentiation and RANKL/OPG ratio in periodontal ligament stem cells by the Wnt/ β -catenin pathway. *Biochimica et Biophysica Acta*, 1860, 2211–2219.
5. Fu, H.D., Wang, B.K., Wan, Z.Q., Lin, H., Chang, M.L. and Han, G.L. (2016) Wnt5a mediated canonical Wnt signaling pathway activation in orthodontic tooth movement: possible role in the tension force-induced bone formation. *Journal of Molecular Histology*, 47, 455–466.
6. Jiang, L. and Tang, Z. (2018) Expression and regulation of the ERK1/2 and p38 MAPK signalling pathways in periodontal tissue remodeling of orthodontic tooth movement. *Molecular Medicine Reports*, 17, 1499–1506.
7. Xu, Y., Shen, J., Muhammed, F.K., Zheng, B., Zhang, Y. and Liu, Y. (2017) Effect of orthodontic force on the expression of PI3K, Akt, and P70S6 K in the human periodontal ligament during orthodontic loading. *Cell Biochemistry and Function*, 35, 372–377.
8. Sun, B., Wen, Y., Wu, X., Zhang, Y., Qiao, X. and Xu, X. (2018) Expression pattern of YAP and TAZ during orthodontic tooth movement in rats. *Journal of Molecular Histology*, 49, 123–131.
9. Ma, J., Zhao, D., Wu, Y., Xu, C. and Zhang, F. (2015) Cyclic stretch induced gene expression of extracellular matrix and adhesion molecules in human periodontal ligament cells. *Archives of Oral Biology*, 60, 447–455.
10. Mattick, J.S. (2004) RNA regulation: a new genetics? *Nature Reviews Genetics*, 5, 316–323.
11. Wei, F.L., Wang, J.H., Ding, G., Yang, S.Y., Li, Y., Hu, Y.J. and Wang, S.L. (2014) Mechanical force-induced specific MicroRNA expression in human periodontal ligament stem cells. *Cells, Tissues, Organs*, 199, 353–363.
12. Chen, N., et al. (2016) microRNA-21 contributes to orthodontic tooth movement. *Journal of Dental Research*, 95, 1425–1433.
13. Chen, Y., Mohammed, A., Oubaidin, M., Evans, C.A., Zhou, X., Luan, X., Diekwiisch, T.G. and Atsawasuwann, P. (2015) Cyclic stretch and compression forces alter microRNA-29 expression of human periodontal ligament cells. *Gene*, 566, 13–17.
14. Ulitsky, I. and Bartel, D.P. (2013) lincRNAs: genomics, evolution, and mechanisms. *Cell*, 154, 26–46.
15. Batista, P.J. and Chang, H.Y. (2013) Long noncoding RNAs: cellular address codes in development and disease. *Cell*, 152, 1298–1307.
16. Wu, J., Zhao, J., Sun, L., Pan, Y., Wang, H. and Zhang, W.B. (2018) Long non-coding RNA H19 mediates mechanical tension-induced osteogenesis of bone marrow mesenchymal stem cells via FAK by sponging miR-138. *Bone*, 108, 62–70.
17. Chen, D., Wu, L., Liu, L., Gong, Q., Zheng, J., Peng, C. and Deng, J. (2017) Comparison of HIF1A-AS1 and HIF1A-AS2 in regulating HIF-1 α and the osteogenic differentiation of PDLCs under hypoxia. *International Journal of Molecular Medicine*, 40, 1529–1536.
18. He, Q., Yang, S., Gu, X., Li, M., Wang, C. and Wei, F. (2018) Long noncoding RNA TUG1 facilitates osteogenic differentiation of periodontal ligament stem cells via interacting with Lin28A. *Cell Death & Disease*, 9, 455.
19. Jia, Q., Jiang, W. and Ni, L. (2015) Down-regulated non-coding RNA (lncRNA-ANCR) promotes osteogenic differentiation of periodontal ligament stem cells. *Archives of Oral Biology*, 60, 234–241.
20. Zheng, Y., Li, X., Huang, Y., Jia, L. and Li, W. (2017) The circular RNA landscape of periodontal ligament stem cells during osteogenesis. *Journal of Periodontology*, 88, 906–914.
21. Zhang, Y.Y., Huang, Y.P., Zhao, H.X., Zhang, T., Chen, F. and Liu, Y. (2017) Cementogenesis is inhibited under a mechanical static compressive force via Piezo1. *The Angle Orthodontist*, 87, 618–624.
22. de Araujo, R.M., Oba, Y., Kuroda, S., Tanaka, E. and Moriyama, K. (2014) RhoE regulates actin cytoskeleton organization in human periodontal ligament cells under mechanical stress. *Archives of Oral Biology*, 59, 187–192.
23. Huang, Y., Zheng, Y., Jia, L. and Li, W. (2015) Long noncoding RNA H19 promotes osteoblast differentiation via TGF- β 1/Smad3/HDAC signaling pathway by deriving miR-675. *Stem Cells*, 33, 3481–3492.
24. Bustin, S.A., et al. (2009) The MIQE guidelines: minimum information for publication of quantitative real-time PCR experiments. *Clinical Chemistry*, 55, 611–622.
25. Kim, D., Langmead, B. and Salzberg, S.L. (2015) HISAT: a fast spliced aligner with low memory requirements. *Nature Methods*, 12, 357–360.

26. Anders, S., Pyl, P.T. and Huber, W. (2015) HTSeq—a Python framework to work with high-throughput sequencing data. *Bioinformatics*, 31, 166–169.
27. Leng, N., Dawson, J.A., Thomson, J.A., Ruotti, V., Rissman, A.I., Smits, B.M., Haag, J.D., Gould, M.N., Stewart, R.M. and Kendziora, C. (2013) EBSeq: an empirical Bayes hierarchical model for inference in RNA-seq experiments. *Bioinformatics*, 29, 1035–1043.
28. Benjamini, Y. and Hochberg, Y. (1995) Controlling the false discovery rate: a practical and powerful approach to multiple testing. *Journal of the Royal Statistical Society Series B (Methodological)*, 57, 289–300.
29. Huang, d.a.W., Sherman, B.T. and Lempicki, R.A. (2009) Systematic and integrative analysis of large gene lists using DAVID bioinformatics resources. *Nature Protocols*, 4, 44–57.
30. Chang, M., Lin, H., Luo, M., Wang, J. and Han, G. (2015) Integrated miRNA and mRNA expression profiling of tension force-induced bone formation in periodontal ligament cells. *In vitro Cellular & Developmental Biology. Animal*, 51, 797–807.
31. Jin, C., Zheng, Y., Huang, Y., Liu, Y., Jia, L. and Zhou, Y. (2017) Long non-coding RNA MIAT knockdown promotes osteogenic differentiation of human adipose-derived stem cells. *Cell Biology International*, 41, 33–41.
32. Jin, C., Jia, L., Huang, Y., Zheng, Y., Du, N., Liu, Y. and Zhou, Y. (2016) Inhibition of lncRNA MIR31HG promotes osteogenic differentiation of human adipose-derived stem cells. *Stem Cells*, 34, 2707–2720.
33. Yao, J., Zhou, B., Zhang, J., Geng, P., Liu, K., Zhu, Y. and Zhu, W. (2014) A new tumor suppressor lncRNA ADAMTS9-AS2 is regulated by DNMT1 and inhibits migration of glioma cells. *Tumour Biology*, 35, 7935–7944.
34. Kirschneck, C., Batschkus, S., Proff, P., Köstlen, J., Spanier, G. and Schröder, A. (2017) Valid gene expression normalization by RT-qPCR in studies on hPDL fibroblasts with focus on orthodontic tooth movement and perodontitis. *Scientific Reports*, 7, 14751.
35. Takewaki, M., et al. (2017) MSC/ECM cellular complexes induce peridental tissue regeneration. *Journal of Dental Research*, 96, 984–991.
36. Ugawa, Y., Yamamoto, T., Kawamura, M., Yamashiro, K., Shimoe, M., Tomikawa, K., Hongo, S., Maeda, H. and Takashiba, S. (2017) Rho-kinase regulates extracellular matrix-mediated osteogenic differentiation of peridental ligament cells. *Cell Biology International*, 41, 651–658.
37. Park, H.J., Baek, K.H., Lee, H.L., Kwon, A., Hwang, H.R., Qadir, A.S., Woo, K.M., Ryoo, H.M. and Baek, J.H. (2011) Hypoxia inducible factor-1 α directly induces the expression of receptor activator of nuclear factor- κ B ligand in periodontal ligament fibroblasts. *Molecules and Cells*, 31, 573–578.